Title

Akt activation disrupts mammary acinar architecture and enhances proliferation in an mTOR-dependent manner.

Journal

The Journal of cell biology, 163(2)

ISSN

0021-9525

Authors

Debnath, Jayanta
Walker, Stephanie J
Brugge, Joan S

Publication Date

2003-10-01

DOI

10.1083/jcb.200304159

Peer reviewed

JCB Article

Akt activation disrupts mammary acinar architecture and enhances proliferation in an mTOR-dependent manner

Jayanta Debnath,[1,2] Stephanie J. Walker,[1] and Joan S. Brugge[1]

[1]Department of Cell Biology, Harvard Medical School, Boston, MA 02115
[2]Department of Pathology, Brigham and Women's Hospital, Boston, MA 02115

Activation of the serine/threonine kinase Akt/PKB positively impacts on three cellular processes relevant to tumor progression: proliferation, survival, and cell size/growth. Using a three-dimensional culture model of MCF-10A mammary cells, we have examined how Akt influences the morphogenesis of polarized epithelial structures. Activation of a conditionally active variant of Akt elicits large, misshapen structures, which primarily arise from the combined effects of Akt on proliferation and cell size. Importantly, Akt activation amplifies proliferation during the early stages of morphogenesis, but cannot overcome signals suppressing proliferation in late-stage cultures. Akt also cooperates with oncoproteins such as cyclin D1 or HPV E7 to promote proliferation and morphogenesis in the absence of growth factors. Pharmacological inhibition of the Akt effector, mammalian target of rapamycin (mTOR), with rapamycin prevents the morphological disruption elicited by Akt activation, including its effect on cell size and number, and the cooperative effect of Akt on oncogene-driven proliferation, indicating that mTOR function is required for the multiple biological effects of Akt activation during morphogenesis.

Introduction

The individual structural units (called acini in the mammary gland) comprising glandular epithelium display remarkable homogeneity in terms of their polarized hollow architecture and uniform size, which critically depends on how epithelial cells interact with each other, with surrounding cells in their microenvironment, as well as with hormones, growth factors, and other cues provided by the extracellular matrix (Bissell and Radisky, 2001). Like all tissue homeostasis, maintenance of these structures requires the tight regulation of growth (cell size), proliferation (cell number), and survival at the level of individual cells (Conlon and Raff, 1999). Disruptions in cell growth, proliferation, and survival are all recognized as key features of oncogenic transformation; however, little is understood about how perturbations of these basic processes within individual epithelial cells ultimately impact on the higher order architecture of a glandular unit (Hanahan and Weinberg, 2000; Bissell and Radisky, 2001).

The culture of epithelial cells on three-dimensional (3D) basement membrane gels promotes their organization into spheroid-shaped structures that share properties with glandular epithelium in vivo; hence, such cultures can be used to address fundamental questions about processes that disrupt epithelial architecture (Streuli et al., 1991; Petersen et al., 1992; O'Brien et al., 2002). For example, we recently found that the induction of constitutive proliferation or inhibition of apoptosis was insufficient to prevent lumen formation during the morphogenesis of mammary acini; rather, the combined disruption of these two processes was required to fill the lumen (Debnath et al., 2002).

While investigating the processes that contribute to lumen formation in mammary acini, we found that matrix-attached cells occupying the periphery of developing acini could be distinguished from centrally localized cells by several criteria. The outer cells display apical–basal polarity and deposit basement membrane components (laminin 5 and collagen IV) on their basal surface, whereas the centrally localized cells do not. Interestingly, we also observed a dichotomy in activation of the serine/threonine kinase Akt/PKB, which was present in a stochastic pattern exclusively in the outer, matrix-attached cells, but not in the centrally located cells that subsequently underwent apoptosis during lumen formation (Debnath et al., 2002). This distinct pattern during acinar development led us to consider whether increased activation

The online version of this article includes supplemental material.

Address correspondence to Joan S. Brugge, Dept. of Cell Biology, Harvard Medical School, 240 Longwood Ave., Boston, MA 02115. Tel.: (617) 432-3974. Fax: (617) 432-3969. email: joan_brugge@hms.harvard.edu

Key words: Akt/PKB; mTOR; mammary acini; cell size; proliferation

Abbreviations used in this paper: 3D, three-dimensional; EHS, Engelbreth-Holm-Swarm; ER, estrogen receptor; ERM, ezrin/radixin/moesin; FKHR-L1, Forkhead ligand 1; mTOR, mammalian target of rapamycin; OHT, 4-hydroxytamoxifen; TSC2, tuberous sclerosis complex 2.

of Akt could promote the survival of cells occupying the luminal space. Akt can regulate cell survival by phosphorylating multiple proteins, including the proapoptotic protein BAD and the Forkhead family of transcription factors (Datta et al., 1997; Brunet et al., 2001). Notably, the PI3K/Akt pathway is activated in a wide spectrum of cancers, due to activation of an upstream growth factor receptor pathway and/or to loss of function of the negative regulatory phosphatase and tumor suppressor protein PTEN (Cantley and Neel, 1999; Vivanco and Sawyers, 2002). Moreover, the increased expression of activated Akt in the mouse mammary gland or brain cooperates with other oncogenic insults to promote tumor formation, presumably due to its ability to increase cell survival (Holland et al., 2000; Hutchinson et al., 2001).

Although the PI3K/Akt pathway is best recognized as a regulator of mammalian cell survival, recent studies have indicated that this pathway controls other critical cellular functions, including proliferation, growth, and metabolism. Notably, Akt can positively impact cell proliferation through numerous signals to the cell cycle machinery and increase cell growth and size by activation of the mammalian target of rapamycin (mTOR) pathway (Lawlor and Alessi, 2001; Abraham, 2002; McManus and Alessi, 2002). How each of these processes actually contributes to the phenotype mediated by PI3K/Akt activation in cancers is an issue of fundamental importance. Moreover, the effects of Akt activation on the formation and maintenance of glandular epithelial structures has not previously been reported, and it remains unclear if specific Akt-regulated processes or pathways are necessary for its phenotypic effects on epithelial architecture. As the PI3K/Akt pathway is often activated in epithelial cancers, this information may be useful in the therapy of carcinomas (Vivanco and Sawyers, 2002).

In this study, we sought to better understand how activation of the PI3K/Akt pathway affects the morphogenesis of epithelial structures by expressing an inducible, activated variant of Akt1 within MCF-10A mammary acini. Akt activation elicits large, misshapen structures, which result from enhanced proliferation and increased cell size, along with variability in size and shape displayed by individual cells within these structures. Remarkably, Akt activation also amplifies the proliferation induced by cyclin D1 or HPV E7 during morphogenesis and cooperates with these oncoproteins to promote proliferation and morphogenesis in the absence of growth factors. Finally, we demonstrate that the effects of Akt activation on morphological disruption, individual cell size and shape, as well as oncogene-driven proliferation are all prevented by rapamycin, a highly specific pharmacological inhibitor of the Akt effector mTOR, suggesting that mTOR is functionally required for all of the phenotype changes elicited by Akt during the morphogenesis of mammary epithelial structures.

Results

Akt activation within mammary acini elicits morphological disruption

To study the effects of Akt activation on acinar morphogenesis, we expressed a conditionally activated variant of Akt in MCF-10A mammary epithelial cells. This previously described version of Akt (hereafter called ER-Akt) consists of a fusion of the Akt1 kinase domain, containing the *src* myristoylation sequence at its NH_2 terminus, to the hormone binding domain of a mutant estrogen receptor (ER) specifically responsive to the estrogen analogue 4-hydroxytamoxifen (OHT) (Kohn et al., 1998). Stable pools of MCF-10A cells expressing ER-Akt were established by retroviral infection. Treatment of these cells (cultured as monolayers) with OHT led to the activation of the Akt chimeric protein, as demonstrated by immunoblotting with antibodies directed against activation-specific phosphorylation sites in Akt (Ser^{473} and Thr^{308}) (Fig. S1, A and B, available at http://www.jcb.org/cgi/content/full/jcb.200304159/DC1); maximal phosphorylation was obtained with 100–1000 nM OHT. OHT treatment increased phosphorylation of several known Akt substrates, including Forkhead ligand 1 (FKHR-L1), tuberin (tuberous sclerosis complex 2 [TSC2]), and glycogen synthase kinase 3 (Fig. S1 C) (Datta et al., 1999; Manning et al., 2002). Activation of the ER-Akt chimera by OHT and the resulting phosphorylation of Akt substrates was significantly inhibited by the PI3K inhibitor LY294002, confirming previous reports that this conditionally active version of Akt is still subject to regulation by PI3K despite the absence of the PIP3-binding pleckstrin homology domain (Fig. S1, B and C) (Kohn et al., 1998). Finally, OHT treatment of ER-Akt–expressing cells led to increased surface expression of GLUT1, a glucose transporter regulated by Akt activation (Fig. S1 D) (Plas et al., 2001; Edinger and Thompson, 2002). Overall, these results demonstrate that activation of ER-Akt in MCF-10A cells induces multiple responses previously shown to be associated with Akt activation.

ER-Akt–expressing MCF-10A cells were cultured on a reconstituted basement membrane gel derived from Engelbreth-Holm-Swarm tumor (EHS; Matrigel™) and treated with either 1 μM OHT or ethanol control (EtOH) starting on day 2 or 3 in 3D culture; cultures were thereafter refed every 4 d. The activation of Akt during morphogenesis led to large, misshapen structures with cells occupying the luminal space (Fig. 1 A, right and center columns). Immunostaining with an antibody that detects phosphorylated Ser^{473} in Akt (αP-Akt Ser^{473}) revealed that high levels of activated Akt were present throughout these structures both in cells with direct matrix contact and in those occupying the luminal space; in contrast, control acini exhibited a stochastic pattern of Akt activation confined to cells in the periphery and similar to that observed in uninfected MCF-10A acini (Debnath et al., 2002).

Individual activated Akt structures displayed varying degrees of morphological disruption and changes in overall structure size. The average diameter of structures from OHT-treated cultures was 112.7 ± 33.2 μm (mean ± SD) versus 61.9 ± 16.3 μm in controls ($P < 0.001$ by *t* test). Evidence of larger size and morphological disruption was evident as early as day 8 in 3D culture and progressively increased thereafter; nevertheless, acini expressing activated ER-Akt did not invade the matrix and continued to secrete the basement membrane protein laminin 5 during morphogenesis (Fig. 1 B).

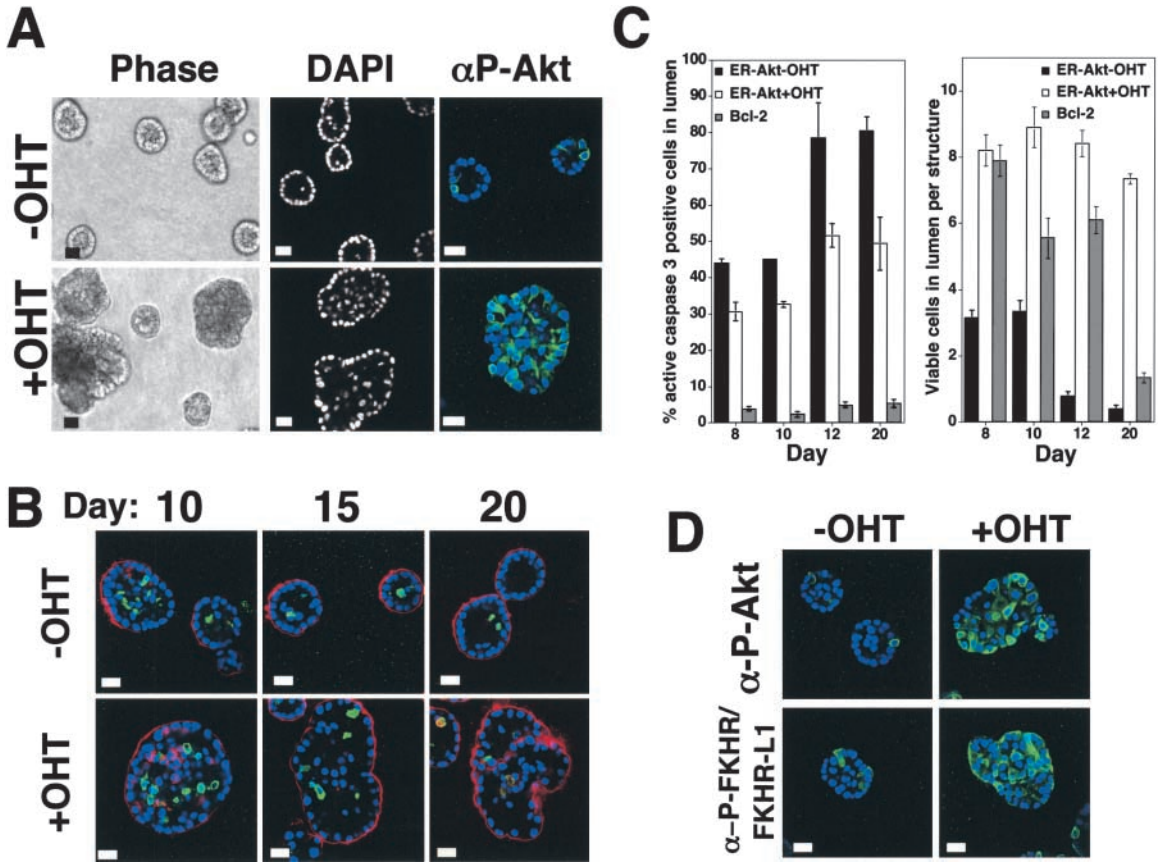

Figure 1. **Effects of Akt activation on mammary acinar morphogenesis and luminal apoptosis.** (A) MCF10A cells expressing ER-Akt were cultured on Matrigel for 15–16 d in the presence of ethanol as vehicle control (top) or 1 μM OHT (bottom). Shown are representative phase images (left), confocal cross sections through the middle of DAPI-stained structures (center), and equatorial DAPI-stained confocal cross sections of structures immunostained with α-phospho Akt Ser^{473} (green, right). Bars, 25 μm. (B) ER-Akt structures grown in 3D with or without 1 μM OHT for the indicated times were immunostained with α-activated caspase 3 (green) and α-laminin 5 (red) and counterstained with DAPI (blue). Shown are equatorial confocal cross sections. Bars, 25 μm. (C) Structures of the indicated cell types were fixed and immunostained as illustrated in B. For both graphs, cells occupying the lumen were defined as those lacking direct contact with basement membrane as delineated by α-laminin 5 staining. (C, left) The percent of cells positive for activated caspase-3 observed in the lumen at various times was quantified; each time point represents the mean ± SD of 90 structures obtained from three independent experiments. (C, right) The mean ± SEM number of viable cells, defined as cells negative for activated caspase-3 present in the lumens of individual structures was enumerated; each time point represents 90 structures obtained from three independent experiments. (D) ER-Akt cells were cultured on EHS for 6 d in the presence of ethanol control (top) or 1 μM OHT and immunostained with α-P-Akt Ser^{473} (green, top) or α-P-FKHR/FKHR-L1 (green, bottom). Shown are equatorial cross sections counterstained with DAPI (blue). Bars, 25 μm.

Akt activation does not completely prevent luminal apoptosis during morphogenesis

We then investigated whether Akt activation affected the induction of apoptosis in the luminal space of mammary structures during morphogenesis by immunostaining with an antibody against the cleaved, activated form of caspase-3 (α-active caspase-3). Surprisingly, we were able to detect significant caspase-3 activation in structures where Akt was activated. As in control acini, the apoptotic cells were confined to those that lacked direct contact with matrix and occupied the luminal space (Fig. 1 B, top). OHT treatment of both wild-type MCF-10A acini and structures only expressing the hormone binding domain of ER did not lead to increased luminal apoptosis, indicating that OHT did not nonspecifically induce apoptosis in the absence of ER-Akt (unpublished data).

Previously, we had shown that lumen formation in MCF-10A acini involved the selective death of centrally located cells during days 8–12 of morphogenesis; thereafter, apoptosis continued to eliminate residual proliferating cells and maintain the hollow lumen (Debnath et al., 2002). Because we observed large numbers of both viable and dying cells in the lumens of active Akt structures throughout morphogenesis, we more closely examined luminal apoptosis in control, active Akt, and Bcl-2-expressing structures at various time points. Indeed, the lumens of active Akt structures contained fewer activated caspase-3–positive cells compared with controls; nevertheless, the protection from apoptosis provided by active Akt was significantly weaker than Bcl-2 (Fig. 1 C, left). Overall, these results indicate that Akt activation can provide partial protection from luminal apoptosis during acinar morphogenesis. Remarkably, both during and after lumen formation, greater numbers of viable cells were observed in the lumen of active Akt structures compared with both control and Bcl-2–expressing structures; in late-stage (day 20) structures, the active Akt structures continued to possess living cells in their luminal spaces, whereas the lu-

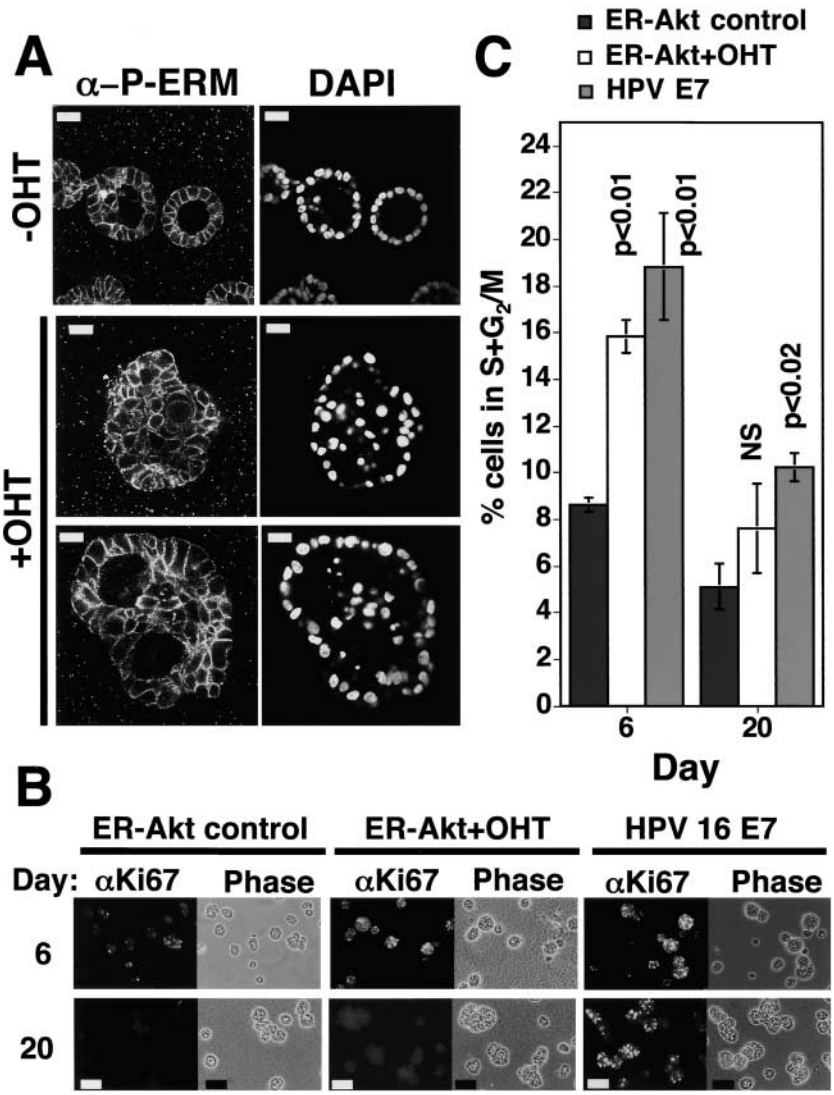

Figure 2. **Cell size and proliferation in activated Akt structures.** (A) After 18 d of 3D culture, structures grown with or without OHT were immunostained with αP-ERM (left), to mark cell membranes to delineate cell size/shape, and DAPI (right). Confocal cross sections through the equators of acini are shown. Bars, 25 μm. (B) Day 6 and 20 acini were immunostained with α-Ki-67. Representative fields show control and OHT-activated Akt structures with occasional Ki-67–positive cells at day 20, while HPV E7–expressing structures continue to proliferate. Corresponding phase contrast images are shown to the right of each Ki-67 stain. Bars, 50 μm. (C) Single cell suspensions of the indicated cell types were prepared from day 6 and 20 cultures, labeled with propidium iodide, and analyzed by flow cytometry to quantify the percent of cells with DNA content corresponding to the S and G2/M (S + G2/M) phases of the cell cycle. The mean ± SEM of three experiments is shown; statistical significance was determined by *t* test, with $P > 0.05$ defined as not significant (NS).

mens of both control and Bcl-2–expressing acini were hollow (Fig. 1 C, right). Finally, we examined the spatial phosphorylation pattern of the Forkhead transcription factors, whose phosphorylation-mediated inactivation is a key mediator of cell survival by Akt (Brunet et al., 2001). α-Phospho-FKHR/FKHR-L1 immunostaining confirmed the increased phosphorylation of Forkhead transcription factors throughout activated Akt structures, while control structures exhibited a stochastic pattern confined to matrix-attached cells (Fig. 1 D, bottom). Hence, the failure of Akt activation to prevent luminal apoptosis could not be explained by the lack of phosphorylation of key Akt-mediated survival effectors in the centrally located cells.

Cell size and proliferation in activated Akt structures

The overall morphological disruption of activated Akt structures and the persistence of cells in the luminal space despite apoptosis in the lumen prompted us to examine if the effects of Akt activation on cell size or cell proliferation contributed to its phenotype. First, we inspected cell size within Akt-activated acini by immunostaining with an antibody against phosphorylated ERM (ezrin/radixin/moesin) proteins (αP-ERM). ERM proteins function as linkers of the plasma membrane to the actin cytoskeleton and are located immediately subjacent to the plasma membrane; hence, we used αP-ERM to outline the plasma membranes in acini and delineate the size and shape of cells within these structures (Bretscher et al., 2000; Debnath et al., 2003). Whereas control acini contained cells with a uniform size and a homogeneous cuboidal shape, cells within activated Akt structures displayed increased size and wide variability in both size and shape (Fig. 2 A). On average, we found a 46% increase in individual cell size within activated Akt structures; the longest linear dimension measured 17.4 ± 6.0 μm versus 11.9 ± 2.8 μm ($P < 0.001$ using *t* test) in controls. In some activated Akt structures, we also observed an increase in size of nuclei of cells; however, we were unable to detect any changes in DNA content by FACS® analysis (Fig. 2 A, bottom right, and not depicted). Based on these results, we postulated that the overall architectural disorganization elicited by Akt activation was at least partially due to the effects of Akt on the size and shape of individual cells comprising these structures.

The phase and DAPI-stained morphology of activated Akt structures indicated that they also contained increased numbers of cells (Fig. 1 A and Fig. 2 A). Hence, we further examined the effects of Akt activation on cell proliferation dur-

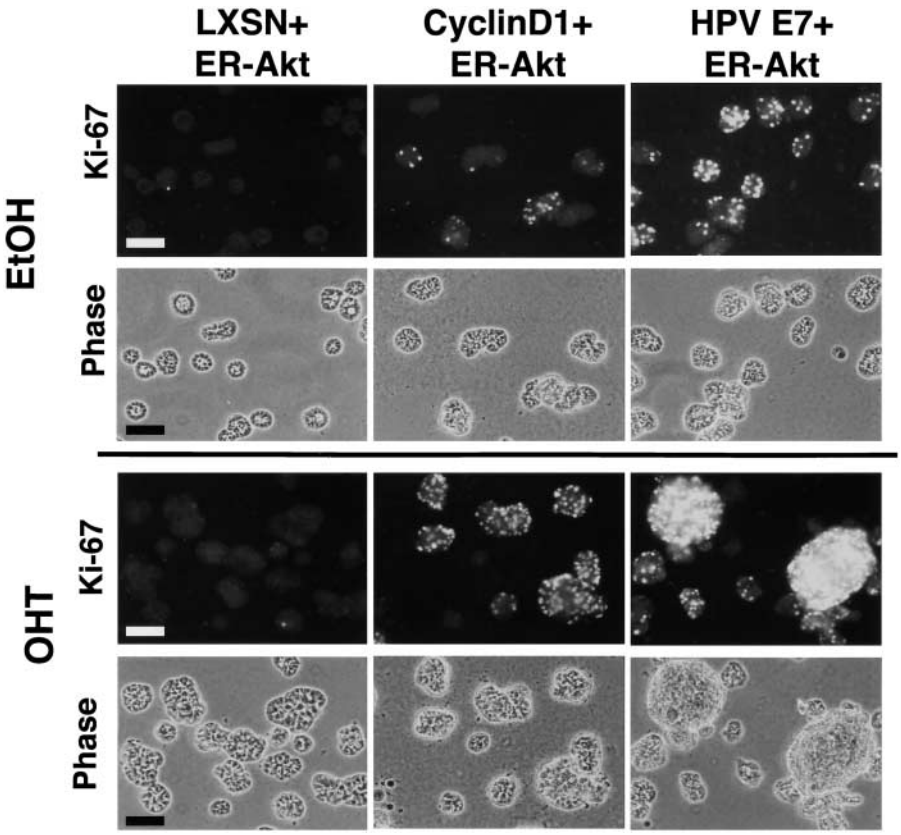

Figure 3. **Akt activation amplifies proliferation in mammary structures coexpressing cyclin D1 and HPV E7.** MCF-10A cells coexpressing ER-Akt with LXSN (vector, left), cyclin D1 (middle), or HPV E7 (right) were cultured on EHS for 20 d with ethanol control (top) or 1 μM OHT (bottom). Representative images of α-Ki-67–immunostained structures along with corresponding phase images are shown. Similar results were obtained with pBABE as the vector control (not depicted). Bars, 50 μm.

ing morphogenesis by immunostaining for the proliferation marker Ki-67 (Scholzen and Gerdes, 2000). Developing MCF-10A acini exhibit high levels of proliferation during the first 6 d of 3D culture; thereafter, Ki-67 activity gradually decreases over the next 10 d. We have previously observed that oncogenes, like cyclin D1, HPV E7, and ErbB2, allow escape from this proliferative suppression (Muthuswamy et al., 2001; Debnath et al., 2002). High levels of Ki-67 activity were detected during the early stages of morphogenesis in both control and OHT-treated ER-Akt–expressing acini. In later stage cultures, structures expressing activated Akt underwent proliferative suppression at a similar rate to controls; only rare Ki-67–positive cells were detected in day 20 cultures (Fig. 2 B). In contrast, acini expressing HPV E7 continued to exhibit high levels of Ki-67 activity in late-stage cultures (Fig. 2 B).

To further investigate proliferation during morphogenesis, cells from 3D cultures corresponding to the early (day 6) and late stages (day 20) of acinar development were harvested, labeled with propidium iodide, and subject to flow cytometric analysis in order to quantify the percentage of cells with a DNA content corresponding to the S and G2/M (S + G2/M) phases of the cell cycle (Fig. 2 C). In day 6 cultures of activated Akt cells, we found an approximately twofold increase versus controls in the percent of cells in S + G2/M. At day 20, Akt-activated cultures exhibited a low percentage of cells in S + G2/M that was not significantly different from controls. In contrast, E7-expressing cells exhibited twofold higher levels of proliferation in both day 6 and day 20 cultures. These results demonstrated that, in contrast to HPV E7, Akt activation did not allow escape from regulatory controls that suppress proliferation during the late stages of morphogenesis in MCF-10A acini (Debnath et al., 2002). Instead, the increased cell number observed in active Akt structures was likely due to enhanced proliferation during the early stages of morphogenesis.

Akt amplifies proliferation in mammary structures expressing proliferative oncogenes

As Akt did not directly affect proliferative suppression during normal morphogenesis, we considered the possibility that Akt activation could enhance proliferation in the context of other cues, such as those provided by growth factors and other cancer genes. Thus, we investigated whether Akt could cooperate with proliferative oncogenes, such as cyclin D1 and HPV E7, in 3D cultures. Stable pools of cells expressing ER-Akt in combination with cyclin D1 and HPV E7 were established and cultured in the absence or presence of OHT. Control acini expressing unactivated ER-Akt along with the empty vector (LXSN) underwent proliferative arrest (Fig. 3, top). Without OHT, cyclin D1 or HPV E7 structures expressing ER-Akt exhibited proliferation in late-stage cultures (day 20) as previously described for structures expressing cyclin D1 or HPV E7 alone (Debnath et al., 2002). Activation of ER-Akt with OHT in cells expressing cyclin D1 or HPV E7 gave rise to structures that were on average larger and that exhibited significantly higher levels of Ki-67 activity than those treated with ethanol control (Fig. 3, bottom).

As previously reported, we detected increased numbers of Ki-67–positive cells with HPV E7 as compared with cyclin D1 in the control cultures (Fig. 3) (Debnath et al., 2002). Interestingly, this difference in Ki-67 activity between these

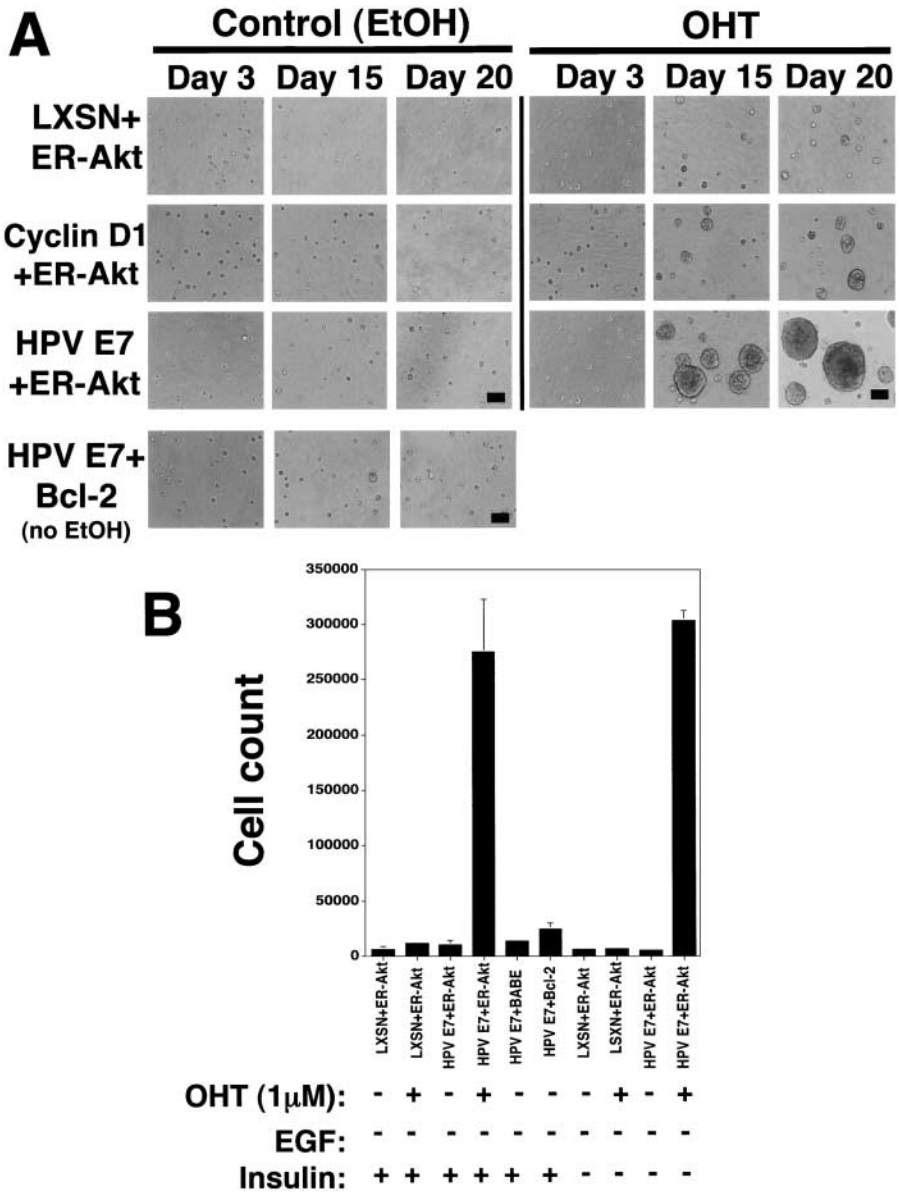

Figure 4. **Akt and HPV E7 cooperate to promote proliferation and morphogenesis in the absence of exogenously provided growth factors.** (A) The indicated cell types were cultured in 3D without EGF along with ethanol control (left) or 1 μM OHT (right) for the indicated number of days; representative phase-contrast images illustrate the development of acinar structures in MCF-10A cells coexpressing cyclin D1 or HPV E7 where ER-Akt has been activated with OHT. Bars, 50 μm. (B) The indicated cell types were cultured in 3D without EGF (or without both EGF and insulin) for 25 d, and cell numbers were quantified. Results represent the mean ± SD from three to five independent experiments.

two oncoproteins was also evident upon OHT-induced activation of ER-Akt; the HPV E7–expressing, Akt-activated structures displayed exceedingly high levels of proliferation compared with all other conditions (Fig. 3). Based on these results, we surmised that Akt could amplify the proliferative events initiated by another stimulus, such as overexpression of oncoproteins like cyclin D1 or HPV E7.

Activated Akt cooperates with proliferative oncogenes to promote proliferation and morphogenesis in the absence of exogenously added growth factors

We further examined the effects of Akt on proliferation by analyzing its ability to promote proliferation and morphogenesis in the absence of added growth factors. Proliferation of MCF-10A cells in monolayers and in 3D cultures is absolutely dependent on exogenously added EGF and insulin (Soule et al., 1990; Muthuswamy et al., 2001). We found that activation of Akt or ectopic expression of cyclin D1 or HPV E7 were insufficient to allow EGF-independent proliferation in Matrigel cultures (Fig. 4, A and B). Only small cell clusters, comprised of three to five cells each, developed over a 25-d period in MCF-10A cultures expressing activated ER-Akt, cyclin D1, or HPV E7 alone, or in vehicle-treated cultures coexpressing the proliferative oncogenes with ER-Akt. (Fig. 4, A and B).

In contrast, when ER-Akt was activated with OHT in cyclin D1–expressing cells, small acinar structures (comprised of 25–30 cells each) developed in the absence of EGF (Fig. 4 A). More strikingly, cells expressing HPV E7 plus active Akt exhibited robust proliferation and morphogenesis during the EGF-independent 3D culture; in these assays, large structures closely resembling those grown in the presence of EGF developed over a 20-d period (Fig. 4 A). Enumeration of cells from these assays revealed a 24-fold increase in the number of cells in cultures of E7 + active Akt cells compared with those expressing E7 alone or those with E7 and unactivated ER-Akt. Moreover, cells with E7 + active Akt were able to proliferate and undergo morphogenesis when

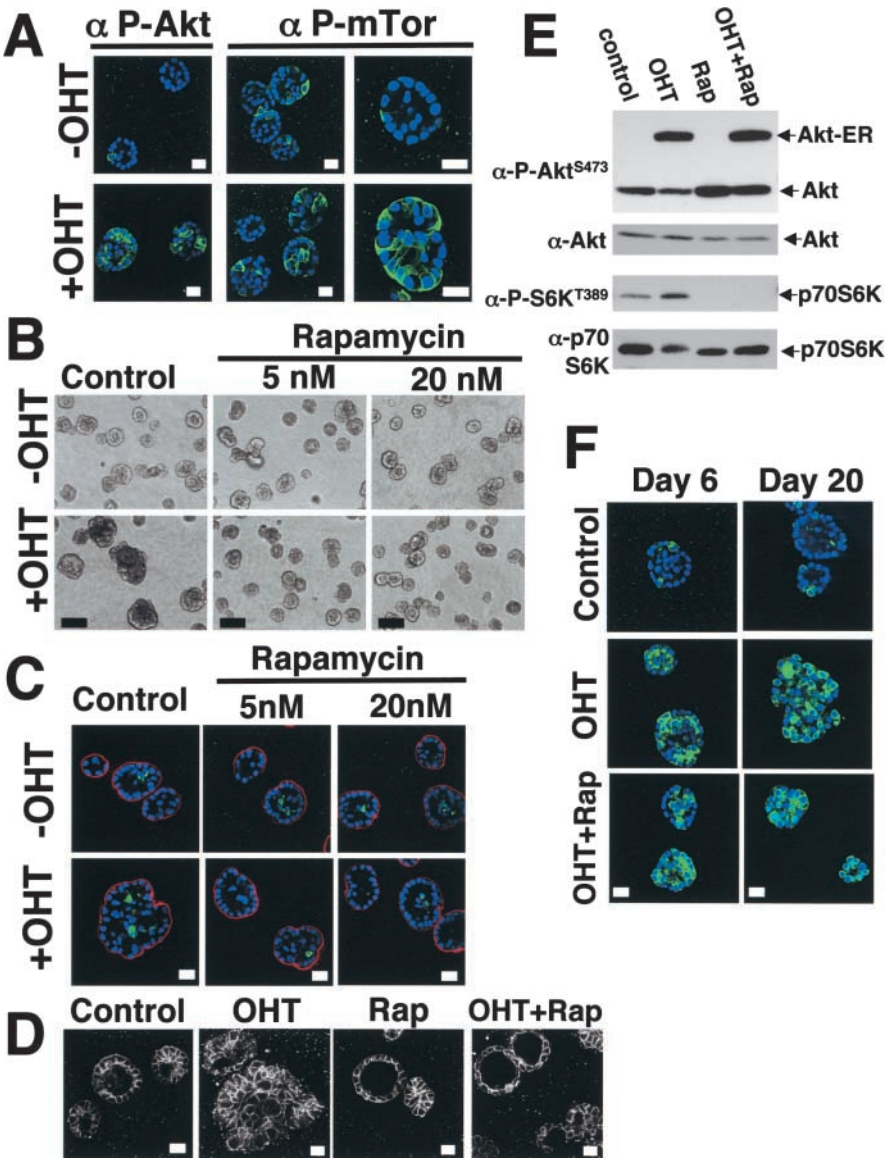

Figure 5. **Rapamycin prevents Akt-mediated disruption of glandular morphology.** (A) ER-Akt cells were cultured on Matrigel for 6 d in the presence of ethanol control (top) or 1 μM OHT; immunostained with α-P-Akt Ser^{473} (green, left) or α-P-mTOR (green, center and right). Shown are DAPI-stained equatorial cross sections. Bars, 25 μm. (B) Phase morphology of day 20 ER-Akt–expressing structures cultured with ethanol control (top) or 1 μM OHT (bottom) along with the indicated doses of rapamycin. Bars, 50 μm. (C) Day 12 ER-Akt structures treated with ethanol control or 1 μM OHT, as well as the indicated doses of rapamycin, were immunostained with α-activated caspase 3 (green) and α-laminin 5 (red). Representative DAPI-stained equatorial confocal cross sections are shown. Bars, 25 μm. (D) Day 20 ER-Akt structures were grown as indicated in the presence of ethanol (control), 1μM OHT, 20 nM rapamycin, or both and immunostained with α-P-ERM to outline cell membranes and illustrate the size and shape of individual cells within these structures. Bar, 25 μm. (E) ER-Akt cells grown as monolayers were treated with OHT (1 μM), rapamycin (20 nM), or both for 6 h, lysed, immunoblotted with α-P-Akt Ser^{473} and α-P-p70S6K Thr^{389}, stripped, and reprobed with α-Akt and α-S6K. (F) ER-Akt structures grown on EHS for the indicated days in vehicle control, 1 μM OHT, or 1 μM OHT + 20 nM rapamycin (Rap) were immunostained with α-P-Akt Ser^{473}; shown are DAPI-stained equatorial confocal cross sections. Bars, 25 μm.

both EGF and insulin were removed from 3D culture (Fig. 4 B). Finally, cells coexpressing HPV E7 and Bcl-2 only formed small clusters in the absence of EGF, indicating that inhibiting apoptosis in E7-containing cells does not mimic the cooperative effect of active Akt and E7 on EGF-independent proliferation and morphogenesis. Altogether, these results indicate that activation of Akt cooperates with proliferative oncogenes to promote both proliferation and morphogenesis in the absence of added growth factors.

We subsequently examined whether the ability of HPV E7 + active Akt cells to proliferate without EGF was due to the production of a secreted mitogenic factor. Control or HPV E7–expressing MCF-10A cells (labeled with Cell-tracker Orange™) were cocultured with MCF-10A cells expressing HPV E7 + active Akt (labeled with GFP). Neither uninfected nor HPV E7–expressing MCF10A cells proliferated when cocultured with HPV E7 + active Akt cells (Fig. S2 A, available at http://www.jcb.org/cgi/content/full/jcb.200304159/DC1, and not depicted). Moreover, in monolayer culture, conditioned media produced from HPV E7 + active Akt cells did not support the proliferation of wild-type MCF-10A cells in the absence of EGF (Fig. S2 B). As a positive control, we generated cells overexpressing a constitutively active variant of the upstream MAPK regulator MEK2 (MEK2 DD); activation of the Erk MAPK pathway via overexpression of Raf can stimulate the production of several secreted factors (TGF-α and HB-EGF) in MCF-10A cells (Schulze et al., 2001). Accordingly, MEK2 DD cells were able to promote the morphogenesis of both uninfected MCF-10A and E7 target cells in 3D culture; also, conditioned media produced from MEK2 DD cells enhanced the EGF-independent proliferation of MCF-10A monolayer cells (Fig. S2, A and B, and not depicted). Thus, while constitutive activation of the Erk MAPK pathway results in the production of secreted growth factors, the effect of Akt activation on growth factor–independent proliferation and morphogenesis involves cell-autonomous mechanisms. Finally, Akt activation was not able to enhance anchorage-independent growth in soft agar, either when expressed alone or in combination with HPV E7, indicating

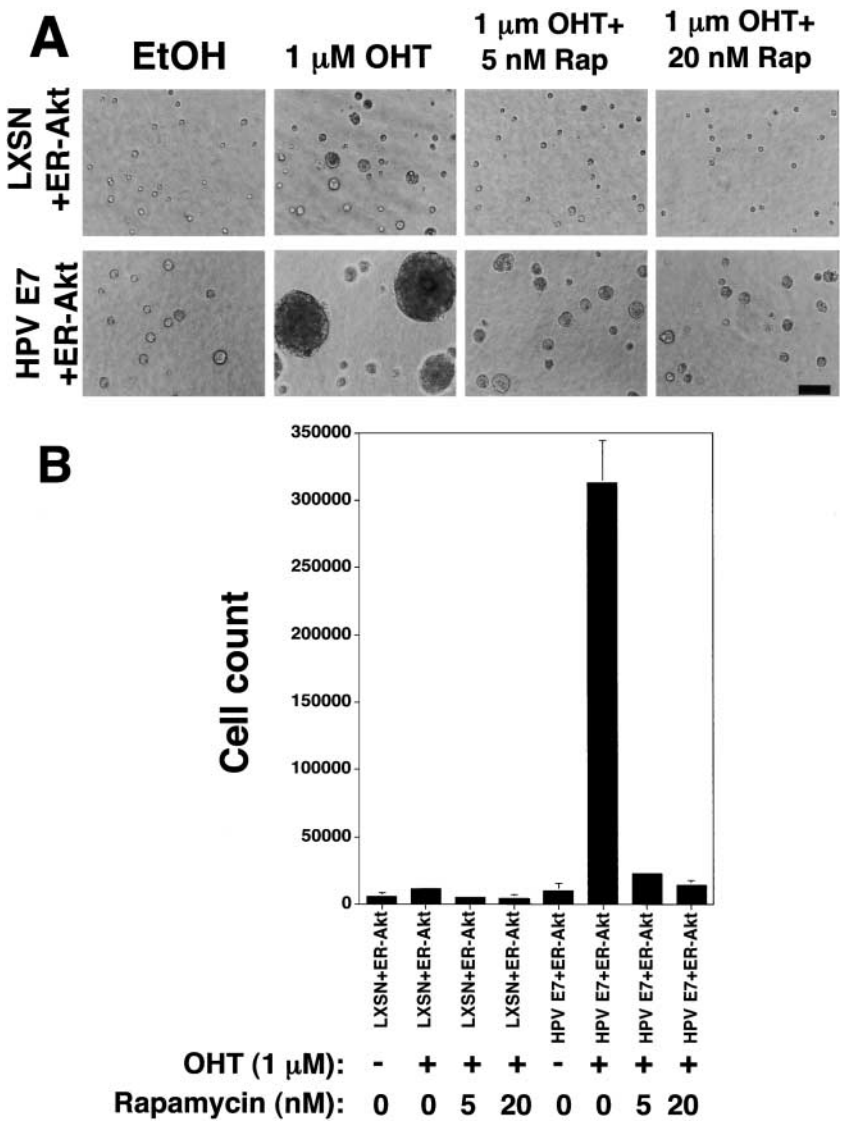

Figure 6. **Rapamycin precludes the cooperative effects of Akt on oncogene-driven, EGF-independent proliferation.** (A) Cells coexpressing ER-Akt along with LXSN (top) or HPV E7 (bottom) were 3D cultured for 20 d in the absence of EGF but with the indicated drug treatments; representative phase-contrast images are shown. Bar, 50 μm. (B) Cells coexpressing ER-Akt with LXSN or HPV E7 were cultured in 3D for 20 d without EGF but with the indicated drug treatments; thereafter, cell numbers were quantified. Results represent the mean ± SD from three independent experiments.

that Akt did not enhance cellular transformation in MCF-10A cells (Fig. S2 C).

mTOR inhibition with rapamycin prevents Akt-mediated disruption of glandular morphology

The combined effects of activated Akt on cell size and proliferation during 3D acinar morphogenesis focused our attention on the role of pathways regulated by mTOR in mediating the phenotype elicited by Akt. Activation of mTOR, and its downstream targets S6K1 (p70S6K) and 4EBP1, has been shown to positively regulate cell size and proliferation in mammalian cells (Wiederrecht et al., 1995; Abraham and Wiederrecht, 1996; Fingar et al., 2002). Abundant evidence has recently indicated that Akt can regulate mTOR function; specifically, the phosphorylation of TSC2 (tuberin) by Akt relieves the inhibitory function of TSC2 on mTOR and, hence, activates downstream signaling (Manning et al., 2002; McManus and Alessi, 2002; Potter et al., 2002; Tee et al., 2002). Accordingly, high levels of phosphorylated mTOR were detected throughout structures in which ER-Akt was activated by OHT; in contrast, control acini exhibited the characteristic stochastic phosphorylation pattern seen with phospho-Akt and phosphorylated Akt substrates (Fig. 5 A) (Debnath et al., 2002). In corroboration, activation of ER-Akt monolayer cells with OHT elicited the phosphorylation of the mTOR regulator TSC2 as well as the downstream mTOR effector p70S6K; however, the phosphospecific antibodies directed toward these molecules were not suitable reagents for the interrogation of 3D cultures (Fig. S1 C and Fig. 5 E).

The macrolide antibiotic rapamycin selectively binds FKBP12 and acts as a highly specific pharmacological inhibitor of mTOR function (Abraham and Wiederrecht, 1996). To elucidate if mTOR is functionally required for the phenotype elicited by Akt, we cultured ER-Akt–expressing cells on basement membrane with OHT along with varying doses of rapamycin, ranging from 1 to 50 nM. At concentrations of 5 nM or higher, rapamycin was able to strongly inhibit the development of large, distorted structures observed with Akt activation in 3D culture (Fig. 5 B). In the presence of rapamycin, activated Akt structures exhibited typical MCF-10A acinar morphology with normal levels of luminal apoptosis (Fig. 5 C). Individual cells within these structures displayed a uniform normal size and cuboidal shape that

phenotypically resembled controls (Fig. 5 D). Furthermore, rapamycin did not adversely affect proliferation or morphogenesis in both uninfected MCF-10A acini and ER-Akt control structures (Fig. 5, B–D, and not depicted). Thus, only activated Akt structures were highly susceptible to the inhibitory effects of rapamycin on mTOR function. Moreover, rapamycin treatment inhibited the phosphorylation of p70S6K, but not Akt or ER-Akt, in OHT-treated monolayer cultures (Fig. 5 E). Also, throughout morphogenesis, ER-Akt structures grown in the presence of both OHT and rapamycin displayed high levels of phosphorylated Akt that were comparable to structures cultured in OHT alone (Fig. 5 F). Overall, these results indicate that mTOR signaling pathways are required for the phenotypic effects mediated by Akt activation during morphogenesis.

Rapamycin inhibits the cooperative effect of Akt on oncogene-driven growth factor–independent proliferation and morphogenesis

As the cooperative influence of Akt activation on HPV E7–driven proliferation in the absence of EGF appeared to involve a cell-autonomous mechanism, we also examined the requirement for mTOR function for this phenotype. Both LXSN + ER-Akt– and HPV E7 + ER-Akt–expressing cells were cultured in Matrigel without EGF, in the presence of OHT, along with varying doses of rapamycin. Rapamycin was able to markedly inhibit EGF-independent morphogenesis of cells with E7 + activated Akt at both the 5 and 20 nM doses; only small clusters developed in these cultures, similar to E7 + ER-Akt controls (Fig. 6 A). Quantification of cell numbers corroborated near complete inhibition of proliferation by HPV E7 + active Akt with rapamycin (Fig. 6 B). Thus, mTOR function is required for the cooperative effect of Akt activation on oncogene-driven proliferation by HPV E7.

Discussion

Activation of Akt in tumor cells enhances tumor cell growth and results in the phosphorylation of numerous substrates, which are believed to positively impact on three major biological processes relevant to cancer progression: cell proliferation (increased cell number), cell growth (increased cell size), and survival (Vivanco and Sawyers, 2002). We have employed the in vitro 3D culture of mammary epithelial cells to explore three principal issues concerning the effect of Akt activation in epithelial cells. First, we have examined how the influence of Akt activation on the aforementioned processes in individual cells impacts on the higher order architecture of polarized epithelial structures. Second, we have attempted to elucidate how these individual cellular processes contribute to the phenotype produced by Akt in both normal and oncogene-expressing structures. Finally, we have investigated the role of mTOR in mediating the Akt-induced effects on acinar architecture.

Most importantly, we have observed that Akt activation enhances proliferation stimulated by growth factors during early morphogenesis, although it is not sufficient to overcome signals causing proliferative arrest, thus limiting the proliferative potential of Akt in 3D structures. Hence, the proliferative signals modulated by Akt are fundamentally distinct from those induced by activated ErbB2, cyclin D1, or HPVE7, which are all able to escape proliferative suppression during morphogenesis (Debnath et al., 2002). The proliferative suppression we have observed in activated Akt structures is consistent with the noticeable absence of hyperplastic lesions in the mammary gland of transgenic mice expressing activated variants of Akt (Hutchinson et al., 2001; Schwertfeger et al., 2001). Moreover, we provide evidence that the proliferative influences of Akt on epithelial cells are primarily cooperative in nature. Indeed, activated Akt significantly amplifies the proliferation provoked by cyclin D1 or HPV E7 during morphogenesis. Moreover, while cyclin D1 and HPV E7 are able to promote constitutive proliferation in MCF-10A acini, this activity is nonetheless EGF driven; remarkably, activated Akt can cooperate with these oncoproteins to promote EGF-independent proliferation and morphogenesis. Akt has been implicated in direct control of cell cycle progression by several mechanisms, including direct phosphorylation-mediated changes in protein stability and subcellular localization of cell cycle inhibitors, $p21^{cip/waf}$ and $p27^{kip}$, and the accumulation of cyclin D1 via phosphorylation-mediated inactivation of glycogen synthase kinase 3β pathway (Diehl et al., 1998; Zhou et al., 2001; Liang et al., 2002; Shin et al., 2002; Viglietto et al., 2002). However, we have been unable to detect changes in the protein levels or subcellular location of any of these proteins upon ER-Akt activation in MCF-10A cells (unpublished data). Rather, our results reveal that mTOR function is required for the cooperative effect of Akt on proliferation, as rapamycin suppresses Akt-induced hyperproliferation.

Our studies also indicate that the effect of Akt on individual cell size and shape may contribute to aberrations in the higher order architecture of epithelial structures. The large distorted structures resulting from Akt activation contain individual cells with increased cell size and a wide variability in cell size and shape. This lack of uniformity among individual cells, the "building blocks" that make up an epithelial acinus, may hinder the assembly of a proper glandular structure. Aberrations in glandular architecture commonly observed in both premalignant and invasive epithelial cancers are notable for both increased cell size and variability in individual cell size and shape; the potential contribution of the PI3K/Akt and mTOR pathways to these histological changes in vivo remains unknown. Notably, our results are similar to those observed upon transgenic overexpression of activated Akt in the mouse prostate, which exhibit hyperplastic, disorganized glands resembling human prostatic intraepithelial neoplasia (Majumder et al., 2003).

Akt-mediated disruption of epithelial cell polarity may also contribute to the morphological changes in acini; however, we have been unable to detect changes in the distribution of several polarity markers in MCF-10A structures. Moreover, we have not observed any alterations in the subcellular location of known polarity regulators (e.g., Discs Large) or in the location of tight junction proteins (e.g., ZO-1) upon activating ER-Akt in Madin-Darby canine kidney 2 polarized monolayers, a commonly used assay for epithelial cell polarity (Knust and Bossinger, 2002; unpublished data). In *Drosophila*, perturbations in Akt expression

affect cell size, which influences the overall compartment size in the imaginal disc (Verdu et al., 1999). Likewise, mutations in *Drosophila* PI3K and TOR pathway components often produce cell size phenotypes, which ultimately impact on organ size or body size (Edgar, 1999). Similarly, transgenic overexpression of activated Akt in the mouse heart results in increased individual size and heart size (Shioi et al., 2002). However, in contrast to our results, the overall architecture of the affected tissues and organs in all of these cases appears intact. The architectural distortion and variability in cell size and shape we have observed could be secondary to local differences in Akt activation within the cells making up these structures. Importantly, the conditionally active Akt variant we have used is subject to regulation by PI3K activity, as treatment of ER-Akt with the PI3K inhibitor Ly294002 significantly reduces its activity. Also, in preliminary studies to monitor PI3K activation using a GFP reporter fused to the pleckstrin homology domain of Akt, we have found a stochastic pattern of PI3K activation within acini resembling that of Akt activation (Hall, A.B., personal communication; unpublished data). Hence, stochastic differences in PI3K activity among individual cells could modulate the activation of ER-Akt and contribute to the variable size and shape changes within cells.

Surprisingly, we have observed that the protection from luminal apoptosis provided by Akt is significantly weaker than the activation of ErbB2 or the overexpression of the antiapoptotic proteins Bcl-2 and Bcl-X_L (Debnath et al., 2002). Nevertheless, several lines of evidence do support a role for Akt in regulating cell survival in mammary epithelium. First, we consistently have detected viable cells within the lumens of activated Akt structures, suggesting that activation of Akt may provide some prosurvival activity. Second, we cannot exclude that local signaling differences within the centrally located cells may regulate the prosurvival activity of Akt in the lumen; although we have clearly demonstrated the increased phosphorylation of Forkhead transcription factors in centrally located cells, the spatial pattern of activation is still stochastic. Hence, individual cells exhibiting reduced levels of Akt activation or Forkhead phosphorylation could still remain susceptible to luminal apoptosis. Finally, in MCF-10A and other epithelial cells, Akt provides significant protection from apoptosis upon detachment from matrix, commonly termed anoikis (Frisch and Francis, 1994; Khwaja et al., 1997; Reginato et al., 2003). Further experiments are needed to clarify the mechanistic basis for the luminal apoptosis that we have observed in activated Akt structures.

Finally, we have found that effects of Akt activation on morphological disruption, proliferation, and cell size and shape are all prevented by rapamycin, a highly specific pharmacological inhibitor of mTOR (Abraham and Wiederrecht, 1996). These results argue that mTOR function is critically required for Akt-mediated phenotypic changes in mammary epithelial structures. Although the precise biochemical relationship between the PI3K/Akt and mTOR signaling pathways remains a subject of intense investigation, recent studies have revealed that Akt can regulate mTOR function by phosphorylating TSC2 (tuberin). This Akt-induced phosphorylation relieves the inhibitory function of TSC2 on mTOR and, hence, activates downstream signaling components (Manning et al., 2002; Potter et al., 2002; Tee et al., 2002). Our results further indicate that the mTOR pathway regulates the effects of Akt activation on both cell size and proliferation. mTOR is believed to regulate cell biosynthesis, growth, and proliferation via its effects on protein translation; modulation of mTOR, and its downstream targets S6K1 and 4EBP1/eIF4E, has been shown to positively regulate both cell size and proliferation in response to both nutrient availability and mitogenic signals (Scott et al., 1998; Sekulic et al., 2000; Rohde et al., 2001; Fingar et al., 2002). Also, recent studies in lymphocytes indicate that the effects of Akt on both cell size and surface expression of nutrient transporters are mTOR dependent (Edinger and Thompson, 2002). How downstream effectors of the mTOR pathway modulate Akt-directed changes during morphogenesis is an important area for further study.

Rapamycin analogues, such as CCI-779, have emerged as potentially important chemotherapeutic agents in cancers because of their high specificity and low systemic toxicity (Abraham, 2002). Rapamycin treatment inhibits focus formation in chicken fibroblasts expressing myristoylated, activated versions of PI3K and Akt; moreover, PTEN-deficient tumor cells display an enhanced sensitivity to CCI-779 in both in vitro and in vivo models (Aoki et al., 2001; Neshat et al., 2001; Podsypanina et al., 2001). Our results corroborate these previous studies and support the further evaluation of rapamycin analogues as chemotherapeutic agents in tumors where the PI3K/Akt pathway has been activated. Moreover, several experimental approaches in this report may serve as tractable biological assays for interrogating Akt functional activity within polarized epithelial structures, and hence, may be useful for the initial in vitro evaluation of new pharmacological agents targeting various components of the PI3K/Akt and mTOR signaling pathways.

Materials and methods

Materials

See supplemental Materials and methods (available at http://www.jcb.org/cgi/content/full/jcb.200304159/DC1) for the sources of cultured cells, chemicals, and antibodies.

Retroviral vectors and virus production

The ER-Akt–expressing retroviral vector, pWZLmyrAkt-HA-ER, was a generous gift from R. Roth (Stanford University, Stanford, CA). pBABEpuro cyclin D1 was constructed from pFLEX cyclin D1 (a gift from A. Diehl, University of Pennsylvania, Philadelphia, PA). pBabepuroMEK2-DD was provided by S. Meloche (University of Montreal, Montreal, Canada). VSV-pseudotyped retroviruses were produced as previously described (Ory et al., 1996). Retroviral vectors encoding HPV 16 E7 and the empty vector (LXSN) were produced from the cell lines PA317-16E7 and PA317-LXSN, respectively, obtained as a gift from D. Galloway (Fred Hutchinson Cancer Research Center, Seattle, WA).

Generation of MCF-10A cell lines

MCF-10A cells (4×10^5 cells) infected with the retroviruses above and stable populations were obtained by selection with 2 μg/ml puromycin (Sigma-Aldrich) or 200 μg/ml G418 (Sigma-Aldrich). Stable pools of MCF-10A cells that coexpressed HPV16 E7 and ER-Akt were generated by serially infecting with HPV16 E7 retrovirus, followed by pWZLmyrAkt-HA-ER; stable pools coexpressing cyclin D1 with ER-Akt were obtained by serial infection of pBABEpuro cyclin D1 followed by pWZLmyrAkt-HA-ER. Protein expression was confirmed by immunoblotting.

Morphogenesis assays

The 3D culture of MCF-10A cells was performed as previously described (Debnath et al., 2003). OHT (1 mM stock) and rapamycin (20 μM stock) were dissolved in ethanol. For ER-Akt activation with OHT, the assay media (DMEM/F12 supplemented with 2% donor horse serum; 5 ng/ml EGF; 10 μg/ml insulin; 100 ng/ml cholera toxin; 0.5 μg/ml hydrocortisone, antibiotics, and 2% Matrigel) was replaced with 1 μM OHT-containing assay media (or ethanol control) starting on day 2 or day 3 of 3D culture and refed every 4 d thereafter. Where indicated, rapamycin was added to cultures at the reported dose on day 2 or 3 of 3D culture and replaced every 4 d thereafter. In 3D morphogenesis assays performed without EGF, or without both EGF and insulin, these reagents were removed as indicated from the assay media described above.

Immunofluorescence analysis and image acquisition

The immunostaining of acinar structures was performed as previously described (Debnath et al., 2003). Indirect immunofluorescent and phase imaging were performed on a Nikon TE300 microscope equipped with a mercury lamp and CCD camera. Confocal analyses were performed using the Carl Zeiss MicroImaging, Inc. LSM410 confocal microscopy system with LSM version 3.99. The images presented represent four or more independent experiments. All images were converted to TIFF format and arranged using Adobe Photoshop 7.0®.

Analysis of cell number and DNA content

To enumerate cell numbers from morphogenesis assays, cultures were treated with 0.5% trypsin, 5 mM EDTA for 30–40 min at 37°C. The trypsin-treated structures were then triturated to generate single cell suspensions, washed, and resuspended in a fixed volume of PBS, and cells were counted using a Beckman Coulter counter or hemacytometer. For flow cytometric analysis of DNA content, single cell suspensions (from 10,000 acini) were prepared as above, fixed in 80% ethanol at 4°C, washed with FACS® buffer (PBS plus 1% FBS), incubated for 30 min at 37°C with 10 μg/ml propidium iodide, 250 μg/ml RNAase A in FACS® buffer, and analyzed on a FACSCalibur® (BD Biosciences) flow cytometer.

Online supplemental material

The supplemental material (Figs. S1 and S2 and supplemental Materials and methods) is available at http://www.jcb.org/cgi/content/full/jcb.200304159/DC1. The data presented in each supplemental figure are described within the text and online legends. Additional experimental details are provided in the supplemental Materials and methods.

We thank Drs. Michael Overholtzer and Mina Bissell for critical reading of the manuscript; Nicole Collins and Dr. Diane Fingar for assistance with flow cytometry; and Drs. Richard Roth, Denise Galloway, Alan Diehl, Sylvain Meloche, and John Blenis for various reagents indicated in the Materials and methods.

This work was supported by the National Cancer Institute (CA80111 and CA89393), Aventis Pharmaceuticals, Department of Defense BCRP (DAMD17-02-1-0692), and the American Cancer Society (to J.S. Brugge); and a Howard Hughes Medical Institute physician postdoctoral fellowship (to J. Debnath).

Submitted: 30 April 2003
Accepted: 8 September 2003

References

Abraham, R.T. 2002. Identification of TOR signaling complexes: more TORC for the cell growth engine. *Cell.* 111:9–12.

Abraham, R.T., and G.J. Wiederrecht. 1996. Immunopharmacology of rapamycin. *Annu. Rev. Immunol.* 14:483–510.

Aoki, M., E. Blazek, and P.K. Vogt. 2001. A role of the kinase mTOR in cellular transformation induced by the oncoproteins P3k and Akt. *Proc. Natl. Acad. Sci. USA.* 98:136–141.

Bissell, M.J., and D. Radisky. 2001. Putting tumours in context. *Nat. Rev. Cancer.* 1:46–54.

Bretscher, A., D. Chambers, R. Nguyen, and D. Reczek. 2000. ERM-Merlin and EBP50 protein families in plasma membrane organization and function. *Annu. Rev. Cell Dev. Biol.* 16:113–143.

Brunet, A., S.R. Datta, and M.E. Greenberg. 2001. Transcription-dependent and -independent control of neuronal survival by the PI3K-Akt signaling pathway. *Curr. Opin. Neurobiol.* 11:297–305.

Cantley, L.C., and B.G. Neel. 1999. New insights into tumor suppression: PTEN suppresses tumor formation by restraining the phosphoinositide 3-kinase/AKT pathway. *Proc. Natl. Acad. Sci. USA.* 96:4240–4245.

Conlon, I., and M. Raff. 1999. Size control in animal development. *Cell.* 96: 235–244.

Datta, S.R., H. Dudek, X. Tao, S. Masters, H. Fu, Y. Gotoh, and M.E. Greenberg. 1997. Akt phosphorylation of BAD couples survival signals to the cell-intrinsic death machinery. *Cell.* 91:231–241.

Datta, S.R., A. Brunet, and M.E. Greenberg. 1999. Cellular survival: a play in three Akts. *Genes Dev.* 13:2905–2927.

Debnath, J., K. Mills, N. Collins, M. Reginato, S. Muthuswamy, and J. Brugge. 2002. The role of apoptosis in creating and maintaining luminal space within normal and oncogene-expressing mammary acini. *Cell.* 111:29–40.

Debnath, J., S. Muthuswamy, and J. Brugge. 2003. Morphogenesis and oncogenesis of MCF-10A mammary epithelial acini grown in three-dimensional basement culture. *Methods.* 30:256–268.

Diehl, J.A., M. Cheng, M.F. Roussel, and C.J. Sherr. 1998. Glycogen synthase kinase-3beta regulates cyclin D1 proteolysis and subcellular localization. *Genes Dev.* 12:3499–3511.

Edgar, B.A. 1999. From small flies come big discoveries about size control. *Nat. Cell Biol.* 1:E191–E193.

Edinger, A.L., and C.B. Thompson. 2002. Akt maintains cell size and survival by increasing mTOR-dependent nutrient uptake. *Mol. Biol. Cell.* 13:2276–2288.

Fingar, D.C., S. Salama, C. Tsou, E. Harlow, and J. Blenis. 2002. Mammalian cell size is controlled by mTOR and its downstream targets S6K1 and 4EBP1/eIF4E. *Genes Dev.* 16:1472–1487.

Frisch, S.M., and H. Francis. 1994. Disruption of epithelial cell–matrix interactions induces apoptosis. *J. Cell Biol.* 124:619–626.

Hanahan, D., and R.A. Weinberg. 2000. The hallmarks of cancer. *Cell.* 100:57–70.

Holland, E.C., J. Celestino, C. Dai, L. Schaefer, R.E. Sawaya, and G.N. Fuller. 2000. Combined activation of Ras and Akt in neural progenitors induces glioblastoma formation in mice. *Nat. Genet.* 25:55–57.

Hutchinson, J., J. Jin, R.D. Cardiff, J.R. Woodgett, and W.J. Muller. 2001. Activation of Akt (protein kinase B) in mammary epithelium provides a critical cell survival signal required for tumor progression. *Mol. Cell. Biol.* 21:2203–2212.

Khwaja, A., P. Rodriguez-Viciana, S. Wennstrom, P.H. Warne, and J. Downward. 1997. Matrix adhesion and Ras transformation both activate a phosphoinositide 3-OH kinase and protein kinase B/Akt cellular survival pathway. *EMBO J.* 16:2783–2793.

Knust, E., and O. Bossinger. 2002. Composition and formation of intercellular junctions in epithelial cells. *Science.* 298:1955–1959.

Kohn, A.D., A. Barthel, K.S. Kovacina, A. Boge, B. Wallach, S.A. Summers, M.J. Birnbaum, P.H. Scott, J.C. Lawrence, Jr., and R.A. Roth. 1998. Construction and characterization of a conditionally active version of the serine/threonine kinase Akt. *J. Biol. Chem.* 273:11937–11943.

Lawlor, M.A., and D.R. Alessi. 2001. PKB/Akt: a key mediator of cell proliferation, survival and insulin responses? *J. Cell Sci.* 114:2903–2910.

Liang, J., J. Zubovitz, T. Petrocelli, R. Kotchetkov, M.K. Connor, K. Han, J.H. Lee, S. Ciarallo, C. Catzavelos, R. Beniston, et al. 2002. PKB/Akt phosphorylates p27, impairs nuclear import of p27 and opposes p27-mediated G1 arrest. *Nat. Med.* 8:1153–1160.

Majumder, P.K., J.J. Yeh, D.J. George, P.G. Febbo, J. Kum, Q. Xue, R. Bikoff, H. Ma, P.W. Kantoff, T.R. Golub, et al. 2003. Prostate intraepithelial neoplasia induced by prostate restricted Akt activation: the MPAKT model. *Proc. Natl. Acad. Sci. USA.* 100:7841–7846.

Manning, B.D., A.R. Tee, M.N. Logsdon, J. Blenis, and L.C. Cantley. 2002. Identification of the tuberous sclerosis complex-2 tumor suppressor gene product tuberin as a target of the phosphoinositide 3-kinase/akt pathway. *Mol. Cell.* 10:151–162.

McManus, E.J., and D.R. Alessi. 2002. TSC1-TSC2: a complex tale of PKB-mediated S6K regulation. *Nat. Cell Biol.* 4:E214–E216.

Muthuswamy, S.K., D. Li, S. Lelievre, M.J. Bissell, and J.S. Brugge. 2001. ErbB2, but not ErbB1, reinitiates proliferation and induces luminal repopulation in epithelial acini. *Nat. Cell Biol.* 3:785–792.

Neshat, M.S., I.K. Mellinghoff, C. Tran, B. Stiles, G. Thomas, R. Petersen, P. Frost, J.J. Gibbons, H. Wu, and C.L. Sawyers. 2001. Enhanced sensitivity of PTEN-deficient tumors to inhibition of FRAP/mTOR. *Proc. Natl. Acad. Sci. USA.* 98:10314–10319.

O'Brien, L.E., M.M. Zegers, and K.E. Mostov. 2002. Opinion: building epithelial architecture: insights from three-dimensional culture models. *Nat. Rev. Mol. Cell Biol.* 3:531–537.

Ory, D.S., B.A. Neugeboren, and R.C. Mulligan. 1996. A stable human-derived packaging cell line for production of high titer retrovirus/vesicular stomatitis

virus G pseudotypes. *Proc. Natl. Acad. Sci. USA.* 93:11400–11406.

Petersen, O.W., L. Ronnov-Jessen, A.R. Howlett, and M.J. Bissell. 1992. Interaction with basement membrane serves to rapidly distinguish growth and differentiation pattern of normal and malignant human breast epithelial cells. *Proc. Natl. Acad. Sci. USA.* 89:9064–9068 (published erratum appears in *Proc. Natl. Acad. Sci. USA.* 1993. 90:2556)

Plas, D.R., S. Talapatra, A.L. Edinger, J.C. Rathmell, and C.B. Thompson. 2001. Akt and Bcl-xL promote growth factor-independent survival through distinct effects on mitochondrial physiology. *J. Biol. Chem.* 276:12041–12048.

Podsypanina, K., R.T. Lee, C. Politis, I. Hennessy, A. Crane, J. Puc, M. Neshat, H. Wang, L. Yang, J. Gibbons, et al. 2001. An inhibitor of mTOR reduces neoplasia and normalizes p70/S6 kinase activity in Pten+/− mice. *Proc. Natl. Acad. Sci. USA.* 98:10320–10325.

Potter, C.J., L.G. Pedraza, and T. Xu. 2002. Akt regulates growth by directly phosphorylating Tsc2. *Nat. Cell Biol.* 4:658–665.

Reginato, M.J., K.R. Mills, J.K. Paulus, D.K. Lynch, D.C. Sgroi, J. Debnath, S.K. Muthuswamy, and J.S. Brugge. 2003. Integrins and EGFR coordinately regulate the pro-apoptotic protein Bim to prevent anoikis. *Nat. Cell Biol.* 5:733–740.

Rohde, J., J. Heitman, and M.E. Cardenas. 2001. The TOR kinases link nutrient sensing to cell growth. *J. Biol. Chem.* 276:9583–9586.

Scholzen, T., and J. Gerdes. 2000. The Ki-67 protein: from the known and the unknown. *J. Cell. Physiol.* 182:311–322.

Schulze, A., K. Lehmann, H.B. Jefferies, M. McMahon, and J. Downward. 2001. Analysis of the transcriptional program induced by Raf in epithelial cells. *Genes Dev.* 15:981–994.

Schwertfeger, K.L., M.M. Richert, and S.M. Anderson. 2001. Mammary gland involution is delayed by activated Akt in transgenic mice. *Mol. Endocrinol.* 15: 867–881.

Scott, P.H., G.J. Brunn, A.D. Kohn, R.A. Roth, and J.C. Lawrence, Jr. 1998. Evidence of insulin-stimulated phosphorylation and activation of the mammalian target of rapamycin mediated by a protein kinase B signaling pathway. *Proc. Natl. Acad. Sci. USA.* 95:7772–7777.

Sekulic, A., C.C. Hudson, J.L. Homme, P. Yin, D.M. Otterness, L.M. Karnitz, and R.T. Abraham. 2000. A direct linkage between the phosphoinositide 3-kinase-AKT signaling pathway and the mammalian target of rapamycin in mitogen-stimulated and transformed cells. *Cancer Res.* 60:3504–3513.

Shin, I., F.M. Yakes, F. Rojo, N.Y. Shin, A.V. Bakin, J. Baselga, and C.L. Arteaga. 2002. PKB/Akt mediates cell-cycle progression by phosphorylation of p27(Kip1) at threonine 157 and modulation of its cellular localization. *Nat. Med.* 8:1145–1152.

Shioi, T., J.R. McMullen, P.M. Kang, P.S. Douglas, T. Obata, T.F. Franke, L.C. Cantley, and S. Izumo. 2002. Akt/protein kinase B promotes organ growth in transgenic mice. *Mol. Cell. Biol.* 22:2799–2809.

Soule, H.D., T.M. Maloney, S.R. Wolman, W.D. Peterson, Jr., R. Brenz, C.M. McGrath, J. Russo, R.J. Pauley, R.F. Jones, and S.C. Brooks. 1990. Isolation and characterization of a spontaneously immortalized human breast epithelial cell line, MCF-10. *Cancer Res.* 50:6075–6086.

Streuli, C.H., N. Bailey, and M.J. Bissell. 1991. Control of mammary epithelial differentiation: basement membrane induces tissue-specific gene expression in the absence of cell–cell interaction and morphological polarity. *J. Cell Biol.* 115:1383–1395.

Tee, A.R., D.C. Fingar, B.D. Manning, D.J. Kwiatkowski, L.C. Cantley, and J. Blenis. 2002. Tuberous sclerosis complex-1 and -2 gene products function together to inhibit mammalian target of rapamycin (mTOR)-mediated downstream signaling. *Proc. Natl. Acad. Sci. USA.* 99:13571–13576.

Verdu, J., M.A. Buratovich, E.L. Wilder, and M.J. Birnbaum. 1999. Cell-autonomous regulation of cell and organ growth in *Drosophila* by Akt/PKB. *Nat. Cell Biol.* 1:500–506.

Viglietto, G., M.L. Motti, P. Bruni, R.M. Melillo, A. D'Alessio, D. Califano, F. Vinci, G. Chiappetta, P. Tsichlis, A. Bellacosa, et al. 2002. Cytoplasmic relocalization and inhibition of the cyclin-dependent kinase inhibitor p27(Kip1) by PKB/Akt-mediated phosphorylation in breast cancer. *Nat. Med.* 8:1136–1144.

Vivanco, I., and C.L. Sawyers. 2002. The phosphatidylinositol 3-kinase AKT pathway in human cancer. *Nat. Rev. Cancer.* 2:489–501.

Wiederrecht, G.J., C.J. Sabers, G.J. Brunn, M.M. Martin, F.J. Dumont, and R.T. Abraham. 1995. Mechanism of action of rapamycin: new insights into the regulation of G1-phase progression in eukaryotic cells. *Prog. Cell Cycle Res.* 1:53–71.

Zhou, B.P., Y. Liao, W. Xia, B. Spohn, M.H. Lee, and M.C. Hung. 2001. Cytoplasmic localization of p21Cip1/WAF1 by Akt-induced phosphorylation in HER-2/neu-overexpressing cells. *Nat. Cell Biol.* 3:245–252.